

Preliminary XFEL Experimental Simulation Platform Based On HSWAP Engine*

LIU Jin¹, DUAN Bowen², WEI Tao¹, KANG Xu¹, ZHAO Shicao², DU Liangliang¹,
DENG Xiaoliang¹, LI Xiaoya¹

(1. National Key Laboratory of Shockwave and Detonation Physics, CAEP, Mianyang 621999, China;

2. Institute of Computer Application, CAEP, Mianyang 621999, Sichuan, China)

Abstract: X-ray Free Electron Laser (XFEL) plays a critical role in diagnosing dynamic compression processes in micro- and meso-scale materials. To deepen our understanding of XFEL physics and optimize facility design, a preliminary XFEL experimental simulation platform was developed based on the High-Performance Computing (HPC) Simulation Workflow Application Platform (HSWAP). HSWAP provides workflow, component, and data linkage models for XFEL experiments, enabling flexible simulation of diverse processes through modular configurations. This platform was employed to investigate X-ray diffraction (XRD) of microscale materials and phase contrast imaging (PCI) of meso-scale explosive samples. Simulation results for XRD of a metallic sample under shock loading and PCI of voids in explosive materials demonstrate the platform's ability to accurately reproduce experimental dynamics. By integrating numerical models with data analysis, the platform enhances the design of XFEL experiments and provides a foundation for interpreting diagnostic capabilities in ultrafast processes. Future work will focus on refining simulation methods for meso-scale samples using phase-field approaches and high-Z materials under shock conditions.

Key words: XFEL experimental simulation platform; HSWAP engine; X-ray diagnostics

CLC number: O521.3

Document code: A

X-ray Free Electron Laser (XFEL) is a high-brightness, ultra-short-pulse x-ray source that has emerged as a transformative tool for studying ultrafast dynamics in micro- and meso-scale materials. XFEL facilities have been established worldwide in the 21st century, including the leading facilities LCLS, SACLA, EuXFEL, and PAL-FEL^[1-9]. The European X-ray Free-Electron Laser (EuXFEL) currently delivers the most intense XFEL pulses, with $>10^{12}$ photons per pulse and a repetition rate of up to 4.5 MHz. The continuous-wave (CW) XFEL model is a growing trend, exemplified by LCLS-II and SFXEL, which operate at frequencies exceeding 1 MHz. XFELs enable the diagnosis of dynamic compression processes in complex materials due to their femtosecond temporal resolution, bridging the gap between microscopic and macroscopic scales. However, the diagnostic capabilities of XFEL for meso-scale systems remain underexplored, particularly in scenarios involving high-velocity shock loading and phase transitions. To address this, simulation platforms such as SIMEX (for experiments at Advanced Laser Light Source)^[10] and Cinema:Bandit (for XFEL shock physics experiments) have been developed^[11].

*Received date: 2025-08-11; Revised date: 2025-10-15

Foundation Item: Fund of National Key Laboratory of Shock Wave and Detonation Physics (JCKYS2022212005)

Corresponding Author: LIU Jin (1978—), male, Ph.D, associate researcher, major in X-ray diagnostic technique. E-mail: ljn_ifp@caep.cn

To address these challenges, this study presents a preliminary XFEL experimental simulation platform based on the HPC Simulation Workflow Application Platform (HSWAP). HSWAP provides a modular framework for integrating numerical models, data processing, and workflow management, enabling the simulation of complex experimental processes in XFEL systems. The platform is designed to facilitate the design of XFEL experiments, optimize facility configurations, and interpret diagnostic signals from meso-scale materials.

This work demonstrates the platform's application in two key areas: (1) X-ray diffraction (XRD) simulations for micro-scale metallic samples under shock loading, and (2) phase contrast imaging (PCI) for meso-scale explosive materials. The results validate the platform's ability to reproduce experimental dynamics and provide insights into the diagnostic capabilities of XFEL. By integrating numerical models and data analysis, the platform offers a systematic approach to advancing XFEL experimental design and understanding the physics of ultrafast processes. Future work will focus on refining simulation methods for meso-scale samples using phase-field approaches and high-Z materials under shock conditions.

1 Simulation Platform

The basic structure of the platform consists of functional modules for different experimental processes, including source generation, X-ray transportation in beamlines, sample evolution, X-ray diagnosing, X-ray detection, and data analysis (Fig.1). For experiments, the physical processes are sequential, so modules are arranged in a sequential manner (Fig.1). All modules are connected via scientific workflows based on the HSWAP engine.

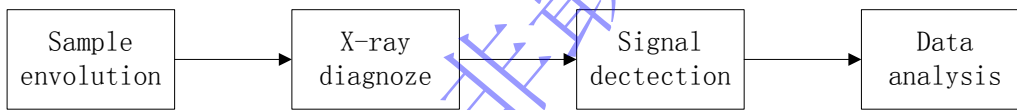


Fig.1 Structure of simulation platform for XFEL experiment

1.1 developed simulation code

1.1.1 Atom-XRD

We developed X-ray diffraction diagnostic simulation program Atom-informed X-ray diffraction (Atom-XRD). In XRD simulation, the elastic scattering of each particle is calculated to obtain the scattered light field $F_i(\mathbf{q})$ [12].

$$F_i(\mathbf{q}) = E \sum_{j=1}^N f_j \exp(2\pi i \mathbf{q} \cdot \mathbf{r}_j) \dots\dots\dots (1)$$

Where \mathbf{q} is the photon momentum transfer, f_j is the structure factor of the particle, \mathbf{r}_j is the spatial coordinate of the atom, N is the total number of atoms in the sample, and E is the incident light field.

In the quantitative process of XRD, two factors are considered.

First, the structure factor f_j . The xraylib functions `'float FF_Rayl'`, `'float Fi'`, and `'float Fii'` are introduced to calculate the scattering length of atoms and convert them into corresponding structure factors [13].

Second, the intensity of the light source. When calculating the superposition of the light field, the differences in light intensity of atoms in different regions are considered. That is, equation (3) is improved to

$$F_i(\mathbf{q}) = \sum_{j=1}^N f_j \exp(2\pi i \mathbf{q} \cdot \mathbf{r}_j) E(\mathbf{r}_j) \quad (2)$$

Where $E(\mathbf{r}_j)$ is the light field at the position of the atom, directly related to the source.

1.1.2 MPCCI

We developed diagnostic simulation program Meso-scale Phase Contrast Imaging (MPCCI) for phase-contrast imaging experiments of meso-scale samples. The program primarily clarifies the relationship between object and image through formulas and the intensity relationship for quantitative calculations. The Fresnel approximation for the propagation of the electromagnetic field is given by

$$\Psi(x, y, z) = \frac{i}{\lambda z} \exp(ikz) \iint \Psi(x', y', 0) \exp\left(\frac{i\pi}{\lambda z} [(x-x')^2 + (y-y')^2]\right) dx' dy' \quad (3)$$

Where $\Psi(x', y', 0), \Psi(x, y, z)$ is the electromagnetic field at sample plane and detector plane, λ is the wavelength of the electromagnetic field, $k = 2\pi / \lambda$. Then consider the electromagnetic field transmitted through the sample from a point source at a distance of ρ_c , we have

$$\Psi(x', y', 0) = T(x', y', 0) \exp(ik\rho_c) \exp\left(\frac{i\pi(x'^2 + y'^2)}{\lambda\rho_c}\right) \quad (4)$$

Where $T(x', y', 0)$ is transmitted factor of the sample. Substituting Equ.(4) into the Equ.(3), we obtained

$$\begin{aligned} \Psi(x, y, z) = & \frac{i}{\lambda z} \exp[ik(z + \rho_c)] \exp\left(\frac{i\pi(x^2 + y^2)(M-1)}{\lambda z M}\right) \\ & \times \iint T(x', y', 0) \exp\left(\frac{i\pi M}{\lambda z} [(x/M - x')^2 + (y/M - y')^2]\right) dx' dy' \end{aligned} \quad (5)$$

where $M = 1 + z / \rho_c$. The equation (5) is transformed into a convolution form, resulting in

$$\begin{aligned} \Psi(x, y, z) = & \frac{i}{\lambda z} \exp[ik(z + \rho_c)] \exp\left(\frac{i\pi(x^2 + y^2)(M-1)}{\lambda z M}\right) \\ & \times \mathbf{F}^{-1} \left\{ \mathbf{F} [T(x', y', 0)] \mathbf{F} \left[\exp\left(\frac{i\pi M}{\lambda z} [(x')^2 + (y')^2]\right) \right] \right\} \end{aligned} \quad (6)$$

Using the Henkel transform relationship, we obtained

$$\begin{aligned} \Psi(x, y, z) = & -\frac{1}{M} \exp[ik(z + \rho_c)] \exp\left(\frac{i\pi(x^2 + y^2)(M-1)}{\lambda z M}\right) \\ & \times \mathbf{F}^{-1} \left\{ \exp(-i\pi\lambda z q^2 / M) \mathbf{F} [T(x', y', 0)] \right\} \end{aligned} \quad (7)$$

1.2 Scientific Workflow

The entire simulation of XFEL experiments involves multiple disciplines and requires a series of related software for collaborative computation. Therefore, these software tools should be integrated to form an integrated application. Scientific workflow technology provides a solution to this problem.

Scientific Workflow (SWF) originated from traditional workflow technology (e.g., Business Workflow, BWF), but unlike business workflows, scientific workflows are data-oriented and feature data

integration, computing integration, and analysis integration. With the development of virtualization platforms and e-Science, scientific workflow technology provides a technical route for co-simulation, offering supporting technology for complex scientific computing processes and automatic operation.

The basic scientific workflow for XFEL simulation connects data, including X-ray wave field data at the end of undulators, X-ray wave field data at the entrance of the station, sample data for X-ray diagnose module as X-ray source, X-ray information after interaction with the sample as input data from X-ray diagnose module to signal detection module, detected signals, and analyzed data sequentially.

1.3 HSWAP engine

For the integrated application of "modeling, computing, analysis, and optimization" in HPC, the HSWAP (Fig.2) engine supports numerical simulation software packaging and workflow design. It constructs a component model based on common operational characteristics of numerical simulations, expresses control and data dependencies via workflows, and establishes a formal numerical simulation workflow model^[14]. The engine adapts to diverse HPC resources, enabling automatic task scheduling and shielding domain users from HPC details. Currently, the engine is deployed in supercomputing centers and supports applications in materials, optics, and mechanics.



Fig.2 Function architecture of HSWAP

The core models of HSWAP engine include workflow model, component model and data link model.

1.3.1 Workflow model

As shown in Fig. 3, HSWAP uses a directed graph $G(A, D)$ to abstract the process of solving complex simulation problems using a series of software as numerical simulation workflow.

A is the simulation activity (Activity), which represents a computation task based on numerical simulation software. An activity includes input ports and output ports, which represent the input and output of the simulation activity. The simulation activity is described by the component model, and its ports are inherited from the input and output ports of the component model.

D is Dependency, including data dependency and control dependency. Data dependency is represented by the matching relationship between data ports (dotted line), which is specifically described by the data link model. The control dependency function $C(A1, A2)$ is defined on control dependency edge (solid line). The function calculates the activation state of the control dependent edge by the simulated activity attributes at both ends of the edge during the execution stage.

Only when the control dependent edge is in active state, the data link process represented by the data dependent edge will be executed during the execution stage, thereby flexibly supporting the expression of control logic such as conditional branches and loops in the numerical simulation process.

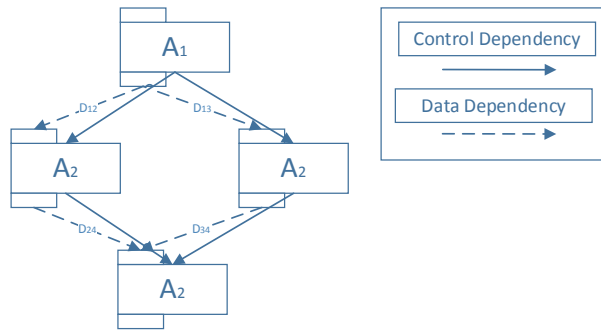


Fig.3 Workflow model in HSWAP

1.3.2 Component model

The component model (as shown in Fig 4) in HSWAP is used to describe the execution process of simulation activities with numerical simulation software as the main part. It encapsulate numerical simulation application software, programs and tools to form functional components. Under the conditions of inputs and outputs being compatible, components can be arbitrarily embedded in the workflow process.

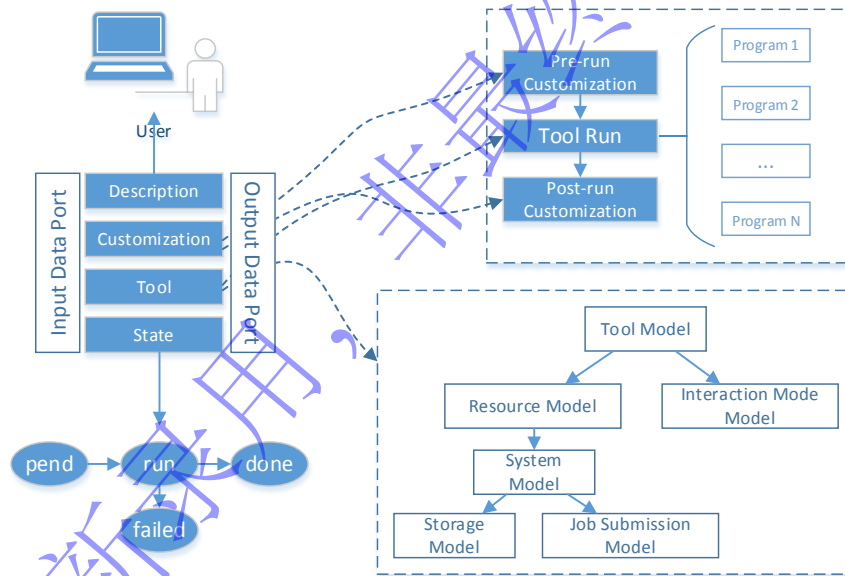


Fig.4 Component model in HSWAP

1.3.3 Data Link Model

The data link model in HSWAP (Fig. 5) is designed for automatic data transfer between simulation activities, and realizes the automatic loose coupling process based on files. The data link model can be represented by a triple (D, O, L) that describes the transformation and transfer of data from the output of one simulation activity to the input of another.

D (Data) is the metadata of the numerical simulation data file, which is represented by (A_id, Path, Port) triplet, representing the activity number, file storage path and data port of the data file respectively. The data port is used to divide by format feature identifiers the multiple input and output files of simulation activities into multiple file sets. The data port is described by (ID, Format, Files), which respectively represent port ID, format description and corresponding file name.

O (Operator) represents the operations for data transmission, including format conversion, data migration, etc.

L (DataLink), indicating the source and destination of data transmission, represented with (S_id, SP_id, T_id, TP_id), respectively indicating the source activity ID, source output port ID, destination activity ID and destination input port ID.

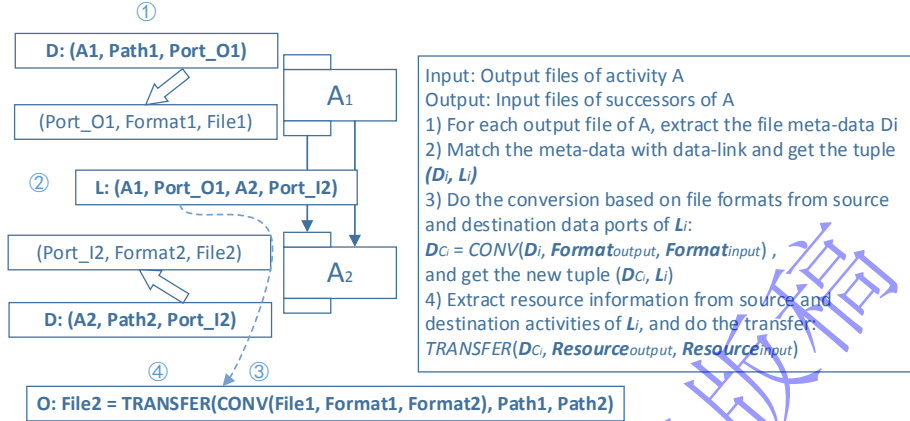


Fig.5 Data link model and execution process of data link in HSWAP

1.4 Integrated

The experimental simulation programs used by the XFEL experimental simulation platform is shown in Table 1. Based on the HSWAP engine, the simulation code are changed to modules, which is like a kind of Programming building block(small squares shown in Fig.6). So the developed XFEL experimental simulation platform gains the ability to flexibly integrate and combine the business in XFEL simulation and form a scientific workflow, forming a preliminary whole-process simulation capability. The simulation programs are integrated as functional components (modules) of the platform and can be combined to form different simulation workflows(Fig.6).

Table 1 Experimental modules for simulation platform

| Physical process | Modules |
|------------------|----------------|
| X-ray diagnosis | Atom-XRD |
| | MPCI |
| Data analysis | XRD-index |
| | Phase-retrieve |

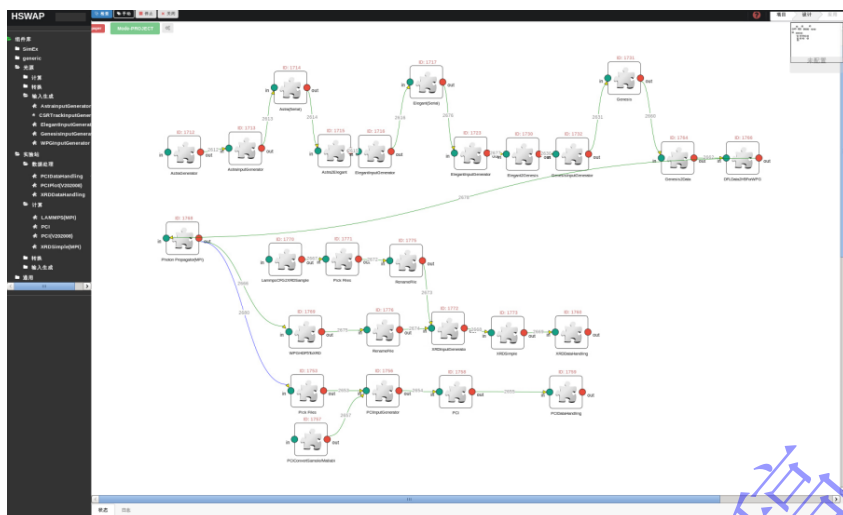


Fig.6 The interface of an XFEL experiment simulation process based on HSWAP engine

2 Application

2.1 Mesoscopic sample thickness for XFEL diagnosis

X-ray intensity attenuation caused by samples constitutes a critical factor in X-ray diagnostic imaging quality. The XFEL facility boosts single-pulse X-ray photon counts by several orders of magnitude, enabling effective imaging with merely 1% intensity attenuation. Through Beer-Lambert law calculations, we determined material-specific thickness thresholds for 1% attenuation at different energy levels (Fig. 7). When a 1 mm thickness induces X-ray intensity to 1%, the requisite X-ray photon energies for sample characterization are 5.67 keV for HXM explorer, 11.54 keV for aluminum, 33.23 keV for iron, and 128.4 keV for tungsten.

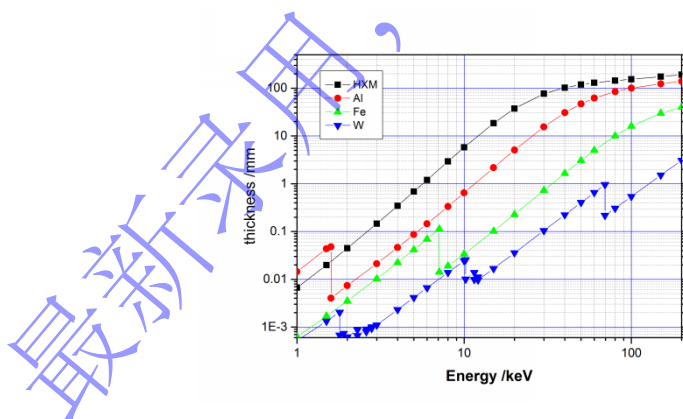


Fig.7 X-ray photon energy versus material thickness curve at 1% attenuation

2.2 XRD Simulation for Micro-Scale Samples

We simulated the dynamic process of a polycrystal iron sample under shock loading with an initial particle velocity of 1.0 km/s along Z-axis. Phase evolution (Fig.8) shows BCC (blue) and HCP (red) phases, with HCP zones expanding with increasing shock times. The XRD pattern was worked out with self-developed codes Atom-XRD of 20 keV XFEL source(Fig.9).The initial XRD peak points (red solid points in Fig.9(a)) faded away gradually with the processes of shock compression. Meanwhile, the width of diffraction line is expanded and some new diffraction peak points with large diffraction angle appeared, which is related to the new phase HCP. This phenomenon is consistent to the molecular dynamic

simulation (Fig.8). This phenomenon is similar to the lattice dynamics experiment under shock-compression at LCLS in the ref[15].

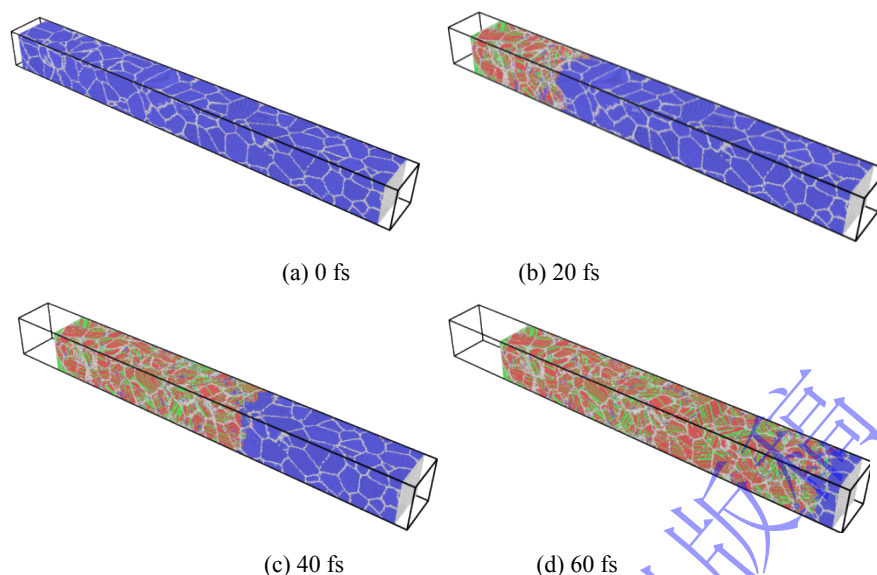


Fig.8 The phase evolution of the Fe sample via times with the initial velocity 1.0 km/s of particles

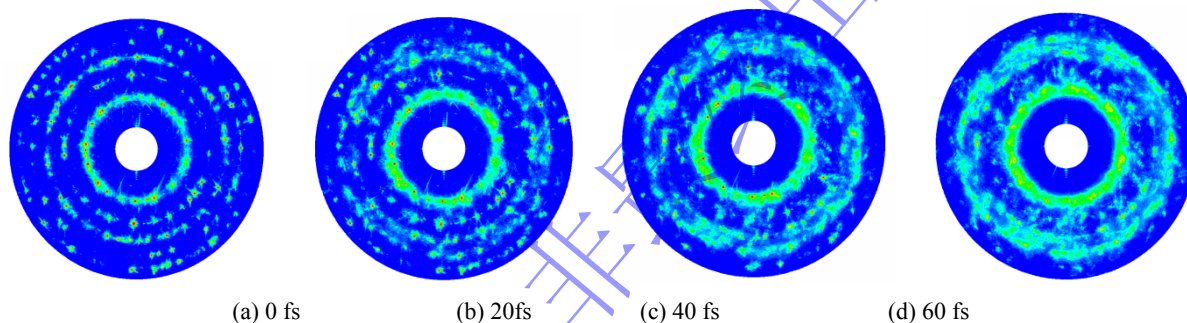


Fig.9 The varied XRD pattern of compressed sample via times

2.3 PCI Simulation for Meso-Scale Samples

The phase contrast imaging to diagnose multiple holes' collapsing processes in explosive under shock loading. The initial sample is size of 1.5 mm*1.5 mm*1.5 mm. Three holes of 300 um diameter is set in the sample(Fig.10 a). The initial velocity of shock wave was set as 600 m/s and the direction is from left to right. The peridynamic code PIC was used to simulate the dynamic collapsing processes for the holes. From the simulation, we found that the shock wave began to compress the above hole at about 0.2 us(Fig.10 b), all three holes are compressed at 0.5 us(Fig.10 c) but the damage of collapse is different, and more interaction time, more damage zone.

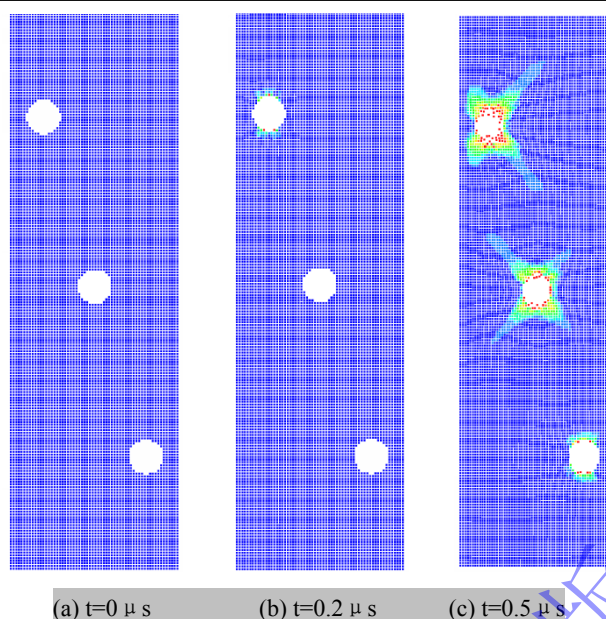


Fig.10 The simulated results of collapsed voids via times (the width of the sample in figure is only about 0.43 mm of the interested zone)

The layout of the PCI system is distance from source to sample 0.7 m, distance from sample to detector 4.9 m. The magnification is 8. The phase contrast images of the collapsed holes were obtained(Fig.11). For explosive is consist of lower Z atoms, the x-ray energy is used as 8.456 keV. In Fig11, the intensive signal zone is becomes smaller consistent to dynamic process, and the edge of the holes were enhanced in a closed line outside of the holes.

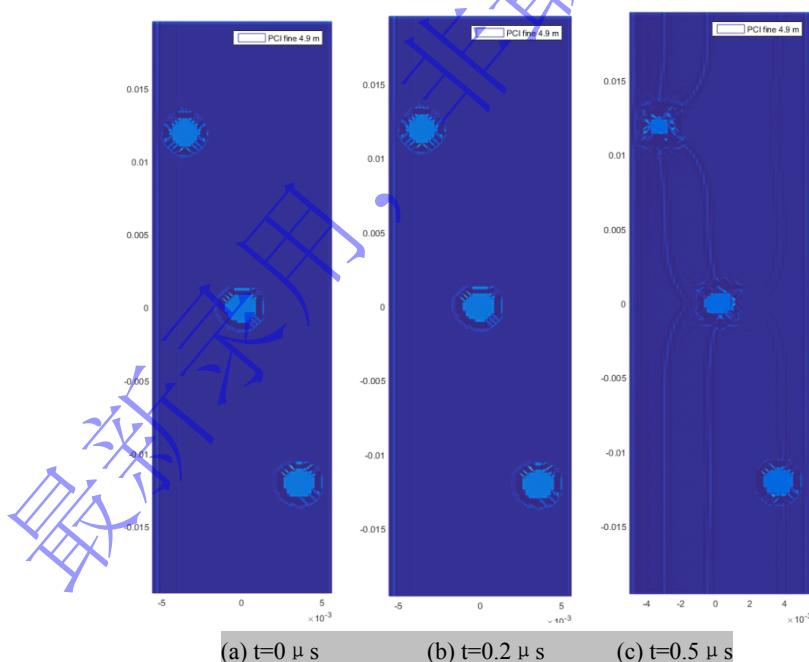


Fig.11 The simulated PCI images of collapsed voids via time

3 Conclusion and discussion

The preliminary XFEL experimental simulation platform, built on the HSWAP engine and scientific workflows, provides capabilities for simulating sample dynamics and diagnosing XFEL x-ray processes. This platform has demonstrated the feasibility of X-ray diffraction (XRD) simulations for micro-scale samples and phase contrast imaging (PCI) for meso-scale explosive materials, supporting XFEL

experiment design and guiding facility development. Future work will focus on integrating phase-field methods for meso-scale XRD simulations and advanced PCI techniques for high-Z materials under shock conditions.

References

- [1] Crabtree G W and Sarrao J L . Opportunities for meso-scale science[J], MRS BULLETIN, 2012,37: 1079-1088.
- [2] Madey J M. Stimulated Emission of Bremsstrahlung in a Periodic Magnetic Field[J], Journal of Applied Physics, 1971,42(5): 1906-1973.
- [3] Akre R , Dowell D , Emma P ,et al.Commissioning the Linac Coherent Light Source injector[J].Review of Modern Physics, 2008, 11(3):347-348.
- [4] Yabashi M. Overview of XFEL and SACLA[J], J. Crystallogr. Soc. Jpn. (Japan) , 2017,59(1):2-5
- [5] Ishikawa T , Aoyagi H , Asaka T ,et al.A compact X-ray free-electron laser emitting in the sub-ngstrm region[J].Nature Photonics, 2012, 6(8):540-544.
- [6] Tschentscher T , Bressler C ,Grünert, Jan,et al.Photon Beam Transport and Scientific Instruments at the European XFEL[J].Applied Sciences, 2017, 7(6):592.
- [7] Abela R , Beaud P , Bokhoven J A V ,et al.Perspective: Opportunities for ultrafast science at SwissFEL[J].Structural Dynamics, 2017, 4(6):061602.
- [8] 陶飞, 张贺, 戚庆林, 等. 数字孪生十问: 分析与思考[J]. 计算机集成制造系统, 2020, 26(1): 1-17. TAO F, ZHANG H, QI Q L, et al. Ten questions towards digital twin: Analysis and thinking[J]. Computer Integrated Manufacturing Systems, 2020, 26(1): 1-17(in Chinese).
- [9] 陶飞, 刘蔚然, 刘检华, 等. 数字孪生及其应用探索[J]. 计算机集成制造系统, 2018, 24(1): 1-16 Fei T , Weiran L , Jianhua L ,et al.Digital twin and its potential application exploration[J].Computer Integrated Manufacturing Systems, 2018, 24(1):1-16(in Chinese).
- [10] Yoon C H , Yurkov M V , Schneidmiller E A ,et al.A comprehensive simulation framework for imaging single particles and biomolecules at the European X-ray Free-Electron Laser[J].Rep, 2016, 6:24791.
- [11] Orban D , Banesh D , Tauxe C ,et al.Cinema:Bandit: a visualization application for beamline science demonstrated on XFEL shock physics experiments[J].Journal of synchrotron radiation, 2020, 27(Pt 1):1-10.
- [12] Als-Nielsen J, McMorrow D. Elements of Modern X-ray Physics[M]. WILEY, 2010.
- [13] Schoonjans T, Brunetti A, Golosio B, et al. The xraylib library for X-ray-matter interactions. Recent developments[J]. Spectrochimica Acta Part B, vol. 66 (2011) :776-784.
- [14] 赵士操,肖永浩,段博文,等.HSWAP:适用于高性能计算环境的数值模拟 workflow 管理平台[J].计算机应用, 2019, 39(6): 1569-1576. Shicao Z , Yonghao X , Bowen D ,et al. HSWAP: numerical simulation workflow management platform suitable for high performance computing environment[J].Journal of Computer Applications, 2019,39(6): 1569-1576(in Chinese).
- [15] Milathianaki D, Boutet S, Williams G J, et al. Femtosecond Visualization of Lattice Dynamics in Shock-Compressed Matter[J].Science,2013, 342 (6155) : 220-223.

基于 HSWAP 引擎的 XFEL 实验模拟平台初探

刘进¹, 段博文², 魏涛¹, 康旭¹, 赵士操², 杜亮亮¹, 邓小良¹, 李晓亚

1

(1. 中国工程物理研究院流体物理研究所冲击波物理与爆轰物理全国重点实验室, 四川 绵阳 621999;

2. 中国工程物理研究院计算机应用研究所, 四川 绵阳 621999)

摘要: X 射线自由电子激光 (X-ray free electron laser, XFEL) 装置是诊断微介观材料动态过程的旗舰装置。为了增强对 XFEL 实验物理的认识能力和装置的设计能力, 利用 HSWAP 工作流管理平台开展了 XFEL 实验模拟平台的研究工作。HSWAP 平台实现了 XFEL 平台的流程模型、组件模型和数据链接模型, 形成初步的 XFEL 实验模拟平台, 并可以方便地使用不同的组件模型创建各种可执行的仿真过程。针对 XFEL 实验中的 X 射线衍射 (X-ray diffraction, XRD) 和相衬成像 (phase contrast imaging, PCI) 诊断技术开展了模拟研究, 实现了分子动力学模拟与 XRD 模拟的结合以及近场动力学计算模拟与 PCI 模拟的结合。通过 XFEL 实验模拟平台的建立和应用, 加深了对 XFEL 诊断能力和实验物理过程的认识。

关键词: XFEL 实验模拟平台; HSWAP 平台; X 光诊断

中图分类号: O521.3

文献标识码: A